

## STUDY OF OPERATIONAL INSTABILITY OF THE RADIAL IMPELLER AND ITS INFLUENCE ON BACKFLOW INDUCED SWIRL

Ignacijo Biluš, Luka Lešnik, Gorazd Bombek  
University of Maribor, Faculty of Mechanical Engineering  
Smetanova ulica 17, Maribor  
Slovenia

### ABSTRACT

The appearance of the swirling flow at the radial impeller entrance is a result of the complicated fluid flow model, which appears as a consequence of the pump operating out of nominal point. Backflow induced swirl has negative effect on efficiency but can cause other disturbances like noise or vibrations too. Due to the complexity of the phenomena it is important to gather as much data about the experiment as possible. The goal of this contribution is to study the capability of the anemometer measuring device and possible contributing factors resulting from the electric motor and fan geometry.

**Keywords:** swirling flow, radial impeller, anemometer, instability, frequency

### 1. INTRODUCTION

The goal of this contribution is to present support activities behind the contribution "Backflow induced swirl at the radial impeller entrance". There is some history and experience in this research field [1]. It is important to know all the frequencies of your system since they can cause resonance [2].

### 2. MEASUREMENT SYSTEM

The measurements of backflow dynamics were performed on a 11-blade radial fan with a tip diameter of  $D = 0.6$  m. The entrance pipe had a diameter of 0.3 m. The anemometer was placed at three entrance pipe diameters in an upstream direction in front of the impeller eye (Fig. 1). The tested fan operated at 1600, 1700 and 1800  $\text{min}^{-1}$  with a flow rate in the range of 0.1–0.8  $\text{m}^3/\text{s}$ .

Vector sensorless frequency generator [3] was used for rotational speed control of 6 kW electric motor.

Measurements of backflow induced swirl were performed using the anemometer with straight blades equipped with RLS RM08 non-contact rotary encoder (1024 pulses per revolution) National instruments 9401 module on 9171 carrier on was used for data acquisition. Optical encoder (5 V) was used for rotational speed measurements.

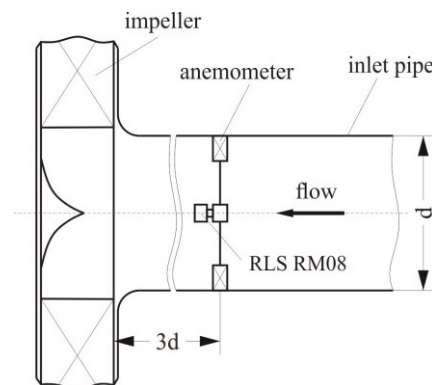


Figure 1. The measurement system

### 3. MEASUREMENT RESULTS

Generally rotational speed measurements are not complicated. But frequency generator and powerful electric motor can cause a lot of noise and disturbances. Optical encoder was used due to its simplicity and ease of assembly. Original plan was to use National Instruments 9401 digital module (8 channels, 100 ns update rate). During testing (manual rotation of the shaft) it was operating normally. Module 9401 uses 5 V digital logic which is suitable for laboratory environment but can be problematic in noisy environment. Our system proved to be unsuited for such an environment and frequencies in 30-33 kHz range were measured. Our second choice was to use NI USB-6255. Original plan was to use counter (for period measurement) and do some extra grounding of the signal. The results were a little better but still unsatisfactory. In the mean time we have discovered that our system works fine when the frequency generator is switched off. So most likely we have found the source of disturbances. Our last attempt was to acquire 30 s of analog signal at 1 MHz sampling rate as presented in Figure 2.

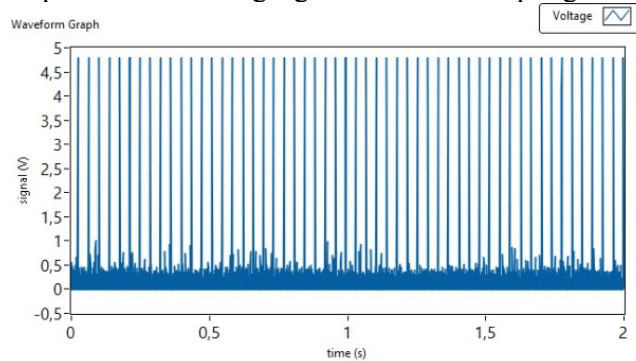


Figure 2. 30 seconds of analog signal

As presented in Figure 2, it is quite simple to analyse the signal and measure time interval between two consecutive pulses as presented in Figure 3.

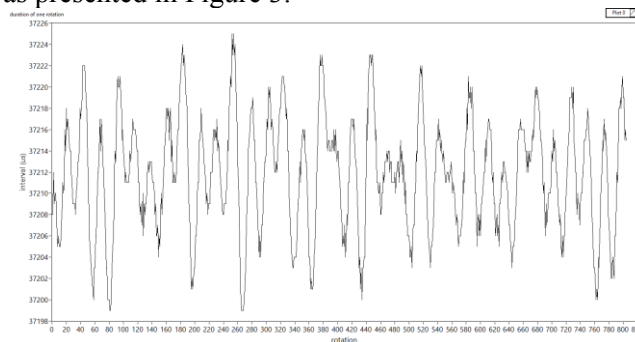


Figure 3. Time interval between pulses

What can be observed from Figure 3? Rotational frequency is not completely stable. Its standard deviation is 0.00014 of its average value so it is possible to conclude that maximum discrepancy ( $3\sigma$ ) of rotational frequency will be less than  $0.7 \text{ min}^{-1}$ . Average rotational frequency of the electric motor proved to be  $1613 \text{ min}^{-1}$  although it was set to 1600. Same kind of pattern can be observed in Figure 4 so the power spectrum of results is presented in Figure 4.

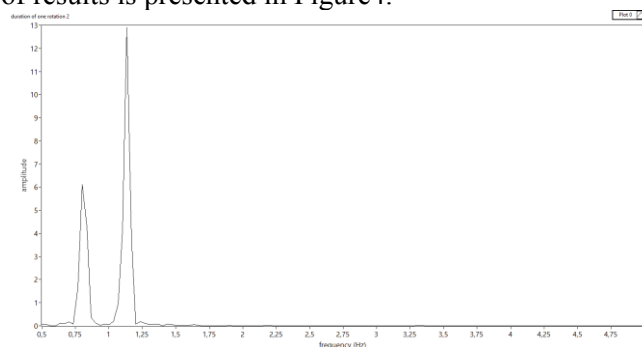


Figure 4. Power spectrum of the results at  $1600 \text{ min}^{-1}$

As can be seen in Figure4, two frequencies can be observed. They are 0.8 and 1.13 Hz. Those frequencies cannot be observed in power spectrum of anemometer signal presented in [4]. Closer look at power spectrum (anemometer signal) acquired at  $Q=0.55 \text{ m}^3/\text{s}$  is presented in Figure5.

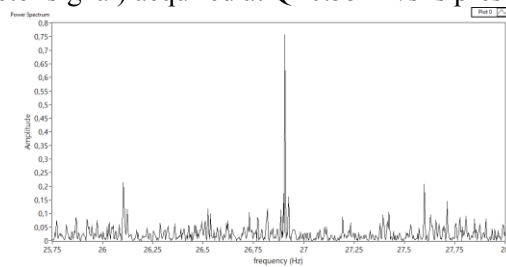


Figure 5. Close-up of frequency spectra at 1600 min-1 0.55 m3/s

Several facts could be observed. First main peak can be located at 26.906 Hz. This corresponds well with the actual rotational frequency of  $1613 \text{ min}^{-1}$ . Two symmetrical minor peaks can be observed at 26.1 Hz and 27.6 Hz. Those peaks can be associated with the change in the rotational frequency. Spectral analysis of the signal presented in Figure2 is presented in Figure4.

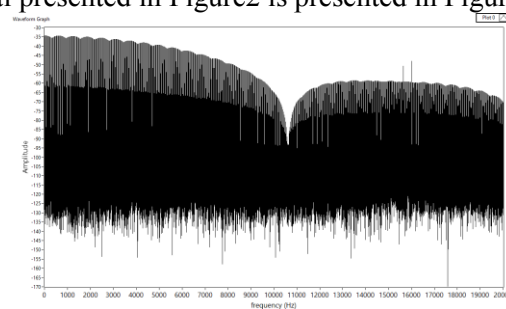


Figure 6. Spectral analysis of the signal (0-20kHz range)

A lot of frequencies can be observed. Frequency of 16 kHz represents the chopping frequency of the frequency generator. Next to it peak at 15677 Hz can be observed. Frequency spectra in 0-800 Hz range is presented in Figure7. Rotational speed and its harmonic frequencies can be observed. Please note that the amplitudes have a pattern which repeats itself after 11 peaks (number of blades).

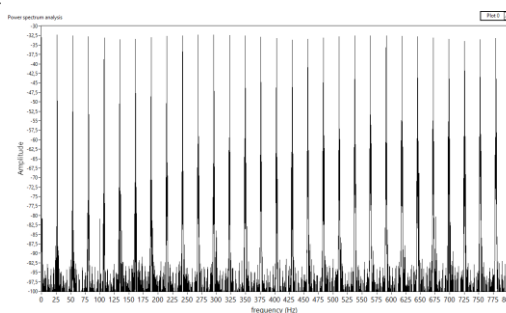


Figure 7. Frequency spectra 0-800 Hz

Closer look at the noise between the peaks in Figure2 is presented in Figure8.

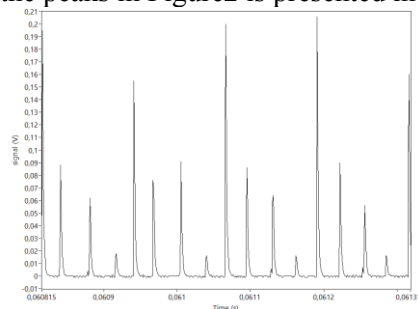


Figure 8. Close-up of the signal between two peaks

Several smaller peaks can be observed in Figure 8. Repetition of each 4-th peak can be seen. Time interval between them is  $125 \mu\text{s}$  (8000 Hz). There are 3 smaller peaks between main peak. It seems that the middle peak lies symmetrically. Main peaks and the middle peaks are caused by frequency generator chopping frequency of 16 kHz. The last peaks are not symmetrical and are most likely associated with the frequency of 15677 Hz. Analog signals were acquired at 1 MHz sampling rate. Digital measurements (NI 9401 and NI USB-6255-period) were performed at 20-40 MHz. The peaks in Figure 8 are very sharp and when problems with digital data acquisition are considered too it is quite possible to assume that the noise peaks could reach approx. 2 V if they were acquired at minimum 10 MHz sampling rate.

Similar procedure was repeated at  $1800 \text{ min}^{-1}$ . Actual average rotational speed was  $1812 \text{ min}^{-1}$ . Its standard deviation was 0,000078 of its mean value. The oscillations were smaller and frequency analysis of rotational speed is presented in Figure 9.

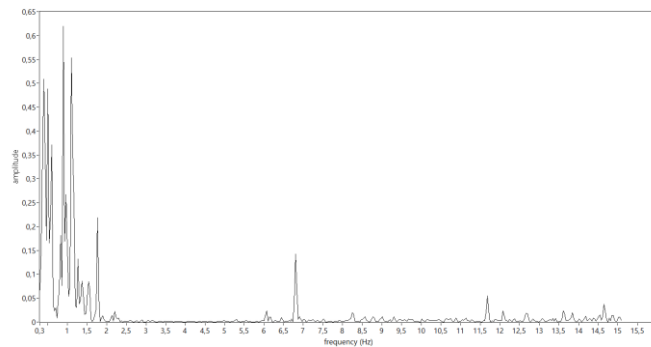


Figure 9. Frequency analysis of rotational speed measurements at  $1800 \text{ min}^{-1}$

No correspondence like the case presented in Figure 5. can be confirmed mostly due to more stable fan rotational speed.

#### 4. CONCLUSION

Stability of fan rotational frequency and its possible influence on backwards induced swirl was analysed in present study. No connection between frequency oscillations and backward induced swirl was found. The results show that frequency controlled electric motor can cause significant electric noise which might cause problems with 5 V digital logic. 24 V digital logic should be used in noisy environments. Filtering could be used to reduce the noise and enable digital data acquisition. Resolution of the results in Figure 3. would be better but filtering could introduce some frequencies which do not exist. The position and electrical connections of the anemometer measurement device was suitable. It was possible to detect oscillations due to instable fan rotational speed and no disturbances due to electric noise were observed. Vector sensorless frequency generators might have minor difference between actual and set rotational speed.

#### 5. REFERENCES

- [1] A. Predin, I. Biluš: Prerotation flow measurement, Flow Measurement and Instrumentation, Vol. 14, p.p. 243-247, 2003.
- [2] Noda, S., et al. Fan noise and Resonance Frequency in Fan-cooled Induction Motors, ForumAcusticum, 2005.
- [3] Jeong, I.-W., et al. Sensorless Vector Control of Induction Motors for Wind Energy Applications Using MRAS and ASO, 2014.
- [4] I. Biluš, G. Bombek, L. Lešnik: Backflow induced swirl at the radial impeller entrance, Proceedings of 21th International Research/Expert Conference TMT 2018, Karlovy Vary, 2018.